THE JOURNAL OF PHYSICAL CHEMISTRY LETTERS
A JOURNAL OF THE AMERICAN CHEMICAL SOCIETY

pubs.acs.org/JPCL

Perspective

Size-Specific Infrared Spectroscopy of Neutral Hydrated Clusters Based on a Vacuum Ultraviolet Free Electron Laser

Gang Li,* Hua Xie, and Ling Jiang*

Cite This: *J. Phys. Chem. Lett.* 2024, 15, 4806−4814

Read Online

ACCESS | Metrics & More | Article Recommendations

ABSTRACT: Spectroscopic study of neutral hydrated clusters provides microscopic insights into the local structures and dynamics of complex systems but is very challenging because of the difficulty in size discrimination. Recently, we developed infrared (IR) spectroscopy based on threshold ionization using a tunable vacuum ultraviolet free electron laser (VUV-FEL). This experimental method allows for size-specific IR spectroscopic measurement of numerous neutral clusters without confinement, such as messenger tags, ultraviolet chromophores, and host matrix. This Perspective aims to highlight the latest advances in VUV-FEL-based IR spectroscopic studies on the confinement-free neutral amine−water, sulfur dioxide−water, and metal−water clusters. Fruitful collaborations with high-level quantum chemical calculations are reviewed. Future research directions with relevance to the atmosphere, biology, and catalysis are proposed.

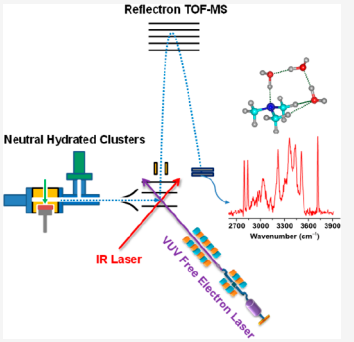

The interactions of water with substances are essential in various areas such as atmospheric new particle formation, biology, and catalysis.[1−3] Spectroscopic measurement of local structures and dynamics remains important and challenging as the vibrational couplings are readily collected to produce diffuse bands that raise the difficulty in the spectral assignment. Gas-phase spectroscopy of hydrated clusters has emerged as an effective strategy for providing detailed information on the microscopic structures and mechanisms of vibrational couplings.[4−8] As exemplified in the simple monohydrated X−H_2O clusters (X = N_2, H_2, CO, CO_2, SO_2, NH_3, HNO_3, H_2SO_4, formamide, benzene, amine, etc.), their quantum tunneling dynamics have been understood via the combination of experimental spectra and theoretical calculations.[7] Studies of ionic hydrated clusters (i.e., $NO_3^-(HNO_3)_n(H_2O)_n$,[9] $H_2PO_4^-(H_2O)_n$,[10] $HCO_2^-(H_2O)_n$,[11] and H^+Pyrimidine-$(H_2O)_n$)[12] revealed large fluctuations of hydrogen bonds (HBs).

Size selection of clusters is an essential prerequisite for the analysis of experimental spectra. Size-specific spectroscopic experiments of charged clusters could be readily achieved via mass spectrometric techniques. Neutral clusters lack charge, which raises the difficulty in detection and size-specific measurement. For small-sized neutral clusters, their experimental spectra could be simple to be analyzed, as shown by matrix-isolation infrared (IR) spectroscopy,[13] microwave, millimeter-wave spectroscopy,[14,15] far-IR vibration−rotation−tunneling spectroscopy,[16] helium-droplet spectroscopy,[17] and angular dependent detection of the scattered beam.[18] While IR−ultraviolet (IR-UV) spectroscopy requires neutral clusters to have a UV chromophore, IR−vacuum ultraviolet (IR-VUV) spectroscopy does not have this requirement. Since the IR-VUV spectroscopy is based on vibrational excitation by an IR laser and ionization detection by a VUV laser, the IR-VUV applicability depends on the wavelength range and pulse energy of the IR and VUV light sources. The recently built vacuum ultraviolet free electron laser (VUV-FEL) features a wide range of tunable wavelength (50−150 nm) and high brightness (the maximum pulse energy >500 μJ).[19]

With the above context, we developed a size-specific IR-VUV spectroscopy instrument (Figure 1A), for which vibrational excitations of neutral clusters are irradiated by a tabletop IR laser (LaserVision) and ionization detections are attained by VUV-FEL threshold photoionization and reflectron time-of-flight mass spectrometer (TOF-MS).[20,21] Two schemes are available to measure the IR spectra of neutral clusters (Figure 1B). (1) IR-VUV depletion scheme: The IR laser is presented at ∼50 ns earlier than that of the VUV-FEL beam. When a vibrational mode of a specific neutral cluster is resonant with the IR laser at a given wavelength, vibrational predissociation would deplete the VUV-ionized TOF-MS signal. Then, IR spectra of this neutral cluster are acquired via the depletion efficiency of VUV-ionized TOF-MS signal intensity by scanning the wavelength of the IR laser. The IR-VUV depletion scheme is applicable to the readily to-be-dissociated neutral clusters with weak binding energies (i.e., water clusters and hydrated clusters). (2) IR+VUV

Received: March 26, 2024
Revised: April 17, 2024
Accepted: April 24, 2024

https://doi.org/10.1021/acs.jpclett.4c00896
J. Phys. Chem. Lett. 2024, 15, 4806−4814

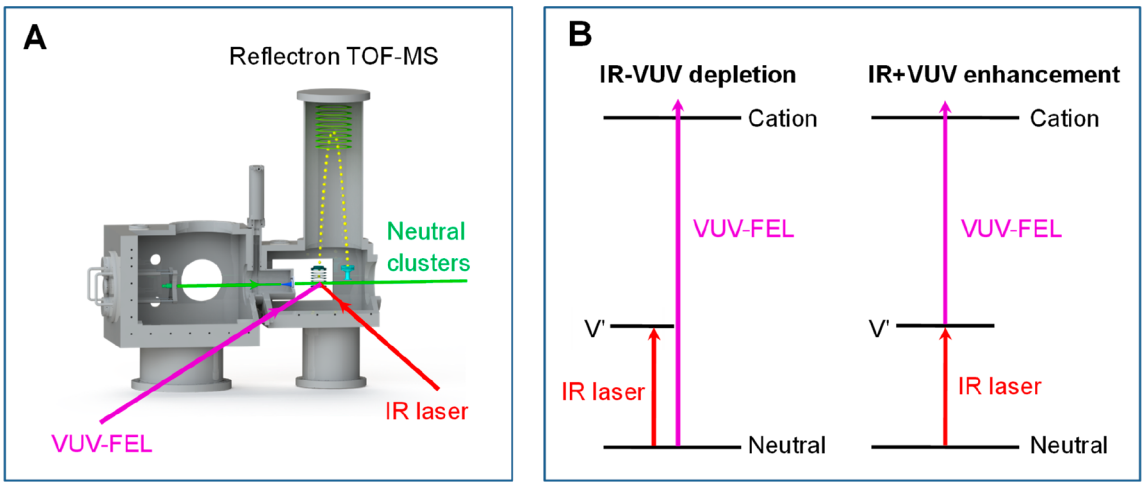

Figure 1. Schematic of the VUV-FEL-based IR spectroscopy instrument (A) and the two experimental schemes (B).

enhancement scheme: The IR laser is also presented at ~50 ns earlier than the VUV-FEL beam. While the VUV-FEL photon energy is slightly below the ionization potential of a specific neutral cluster, neutral clusters resonantly absorb a few IR photons, leading to the enhancement of the VUV ionization efficiency. IR spectra of this neutral cluster are thus obtained via the enhancement efficiency of the VUV-ionized TOF-MS signal intensity by scanning the wavelength of the IR laser. The IR +VUV enhancement scheme is applicable to difficult-to-be-dissociated neutral clusters with strong binding energies (i.e., metal clusters).

Since the VUV-FEL wavelength range (50−150 nm, 8.3−24.8 eV) covers the first ionization potentials of a broad range of neutral clusters, it is promising to attain the size-specific IR spectra of numerous neutral clusters without environmental perturbation (i.e., a messenger tag, an ultraviolet chromophore, or a host matrix).[20−22] With this VUV-FEL-based IR method, we have succeeded in a series of size-specific spectroscopic studies of neutral hydrated clusters,[23−28] water clusters,[29−33] ammonia clusters,[34] and metal carbonyls.[35−38] This Perspective highlights recent VUV-FEL-based size-specific IR spectroscopic studies of neutral hydrated clusters, such as amine−water, sulfur dioxide−water, and metal−water complexes. These examples show ample demonstrations of scientific opportunities enabled by the use of VUV-FEL. Future research themes of VUV-FEL-based size-specific IR spectroscopic studies are proposed.

Amines are known to enhance the nucleation and growth of atmospheric new particles.[1,39] Considering that trimethylamine (TMA) is one of the amines having the largest proton affinities (~949 kJ/mol) with a preference to form strong hydrogen bonds, the trimethylamine−water clusters are thus chosen as a model of an amine−water system in this work. Figure 2 shows the experimental IR-VUV depletion spectra of neutral TMA-$(H_2O)_n$ with n = 1 through 3. Table 1 lists the peak positions and assignments. IR spectra for n = 1 were measured at 131.00 nm, for n = 2 at 132.00 nm, and for n = 3 at 133.00 nm, respectively. Experimental details could be found in a brief report of the n = 1 cluster.[23] The IR spectrum of the n = 1 cluster contains six groups of peaks (labeled A−F), which exhibit six HB-ed OH stretching peaks (B_1−B_6). Such strong dynamic couplings arise from the Fermi resonance among the HB-ed OH stretching modes and the water bend, rock, and translation motions, as interpreted by a theory combination of quantum mechanical calculations with multidimensional ab initio potential energy

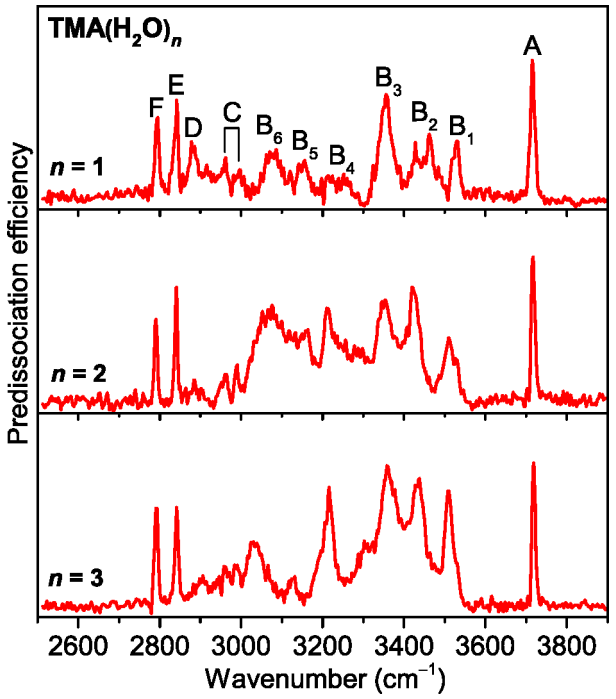

Figure 2. Experimental VUV-FEL-based IR spectra of neutral TMA$(H_2O)_n$ clusters with n = 1 through 3.

surfaces, discrete variable representation (DVR) anharmonic algorithm, and ab initio molecular dynamics (AIMD).[23]

Spectral features of TMA$(H_2O)_n$ (n = 2 and 3) are similar to those of n = 1, with slight changes in peak positions, intensities, and widths. Peak A slightly blue shifts from 3715 cm^{-1} at n = 1 to 3717 cm^{-1} at n = 2 and to 3719 cm^{-1} at n = 3, which gradually gets closer to the antisymmetric OH stretching frequency of free H_2O (3756 cm^{-1}), indicative of a slight recovering of bonding electron densities of the free OH groups with increasing H_2O number. The progression of several broadened peaks with intensity modulation in the 3000−3600 cm^{-1} region is observed for all of the clusters studied here. The positions of the C−F peaks (the CH stretching modes) are not sensitive to the cluster size, which is consistent with the previous observation of little vibrational coupling between the CH_3 and OH groups.[23] Interestingly, the broad progression of HB-ed OH stretching modes (B_1−B_6) appears in the IR spectra of larger clusters n = 2

https://doi.org/10.1021/acs.jpclett.4c00896
J. Phys. Chem. Lett. 2024, 15, 4806−4814

Table 1. Experimental IR Peaks (in cm^{-1}) and Assignments of $TMA(H_2O)_n$ with $n = 1-3$

Label	$n = 1$	$n = 2$	$n = 3$	Assignment
A	3715	3717	3719	Free OH stretch
B_1	3530	3510	3510	Coupling among HB-ed OH stretch, water bend overtone, intermolecular translation, intermolecular water in-plane, and out-of-plane rocks
B_2	3462	3420	3438	
B_3	3356	3356	3358	
B_4	3210	3210	3216	
B_5	3156	3154	3132	
B_6	3086	3073	3035	
C	2992	2990	2988	Antisymmetric CH stretch
	2962	2958	2958	
D	2885	2883	2882	Combination of two CH_3 bends
E	2842	2842	2842	Coupling of symmetric/antisymmetric CH stretches with overtones of CH_3 bend and CH_3 umbrella
F	2795	2793	2793	Coupling of symmetric CH stretch with overtones of CH_3 bend and CH_3 umbrella

and 3, indicating that large fluctuations of HBs still persist even when the water molecules increase. Considering that the assignments of the A−F peaks have been discussed in a previous report of $n = 1$,[23] we will focus on the evolution of dynamic couplings of HBs with the cluster size.

The MP2/aug-cc-pVDZ calculations were carried out to address the structures and spectra of the $TMA(H_2O)_n$ clusters.[23] The harmonic frequencies are scaled by 0.959. The global minimum structures and corresponding harmonic vibrational spectra are shown in Figure 3. In the most stable isomer of $n = 2$

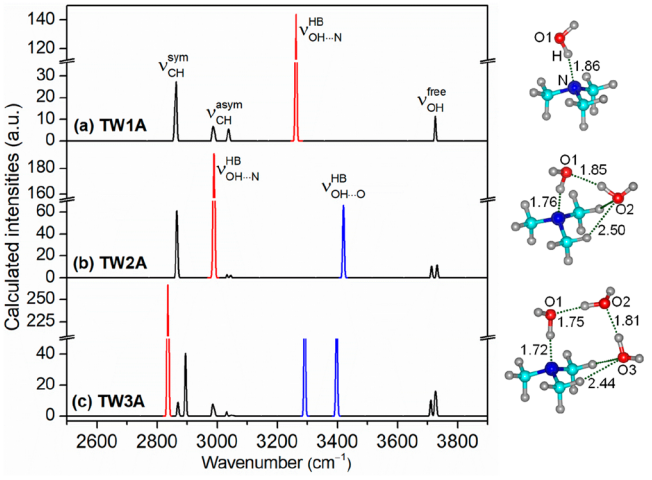

Figure 3. Calculated harmonic vibrational spectra of the most stable isomers of $TMA(H_2O)_n$ ($n = 1-3$). The structures are illustrated (O, red; N, blue; C, cyan; H, light gray). The HB distances are indicated in angstrom.

(labeled TW2A), the second water molecule forms one O···HO bond with the first water molecule and two weak H···OH bonds with the CH_3 groups of TMA. The most stable isomer of the $n = 3$ cluster (TW3A) consists of a water chain.

The free OH stretches (ν_{OH}^{free}) in the TW1A, TW2A, and TW3A isomers are predicted at ~3726 cm^{-1} (Figure 3), which are in accord with the experimental values (3715−3719 cm^{-1}). The stretch of the OH group that is HB-ed to the N atom of TMA ($\nu_{OH\cdots N}^{HB}$) in the TW1A, TW2A, and TW3A isomers is calculated to be 3262, 2990, and 2836 cm^{-1}, respectively, reflecting a gradual stregthening of the N···HO bond with the increase of cluster size, as indicated by the N···HO bond distances shortened from 1.86 Å at $n = 1$ to 1.72 Å at $n = 3$ (Figure 3). The stretch of the OH group that is HB-ed to the O atom of water ($\nu_{OH\cdots O}^{HB}$) in TW2A and TW3A is predicted at 3420 and 3292/3397 cm^{-1}, respectively, indicating a smaller red shift as compared to the $\nu_{OH\cdots N}^{HB}$.

To elucidate the fluctuation extent of HBs in the $TMA(H_2O)_n$ ($n = 1-3$) clusters and its consequence for the vibrational features, AIMD simulations at finite temperatures were carried out for the TW1A, TW2A, and TW3A isomers.[23] The AIMD simulated spectra of isomers TW1A, TW2A, and TW3A are summarized in Figure 4. For TW1A, the phase space is better

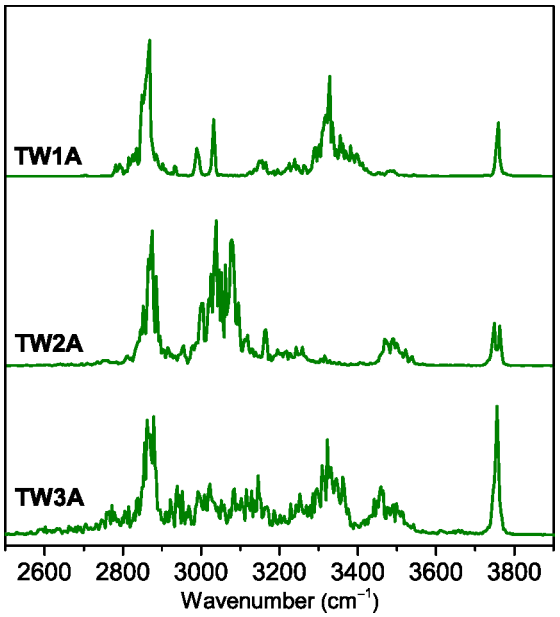

Figure 4. AIMD calculated spectra of isomers TW1A (250 K), TW2A (200 K), and TW3A (200 K).

sampled at 250 K, yielding a simulated spectrum that is in agreement with the experimental one. For TW2A and TW3A, the fluctuation of the N···HO bond is more rigid due to the HB network formation between water molecules and TMA, as indicated by a gradually shortened N···HO bond length with growing cluster size (Figure 3). The AIMD simulated spectra of TW2A and TW3A at 200 K are found to agree better with the experimental spectra.

The fluctuations in the N···H and O···H bond distances of isomers TW1A, TW2A, and TW3A are illustrated in Figure 5. The variation of N···H bond distances in TW1A is in the range of 1.6−2.5 Å, and those in TW2A and TW3A are in the range of 1.5−2.2 Å. Similarly, considerable fluctuations (1.6−2.4 Å) in the O···H bond distances are also predicted during the AIMD runs. These results indicate that large fluctuations of HBs still persist in the $n = 2$ and 3 clusters. Such dynamic fluctuations induce substantial shifts in the OH stretching frequencies, which then lead to the observed series of diffuse OH stretching peaks (B_1-B_6).

As listed in Table 2, in the TW1A isomer, the $\nu_{OH\cdots N}^{HB}$ (3262 cm^{-1}) is very close to $2\delta_{OH\cdots N}$ (3200 cm^{-1}), and the OH bend overtone readily borrows the intensity from the HB-ed OH stretch. In the TW2A isomer, $\nu_{OH\cdots N}^{HB}$ is lower than the $2\delta_{OH\cdots N}$ by 240 cm^{-1}, for which the OH bend overtone still manages to

https://doi.org/10.1021/acs.jpclett.4c00896
J. Phys. Chem. Lett. 2024, 15, 4806−4814

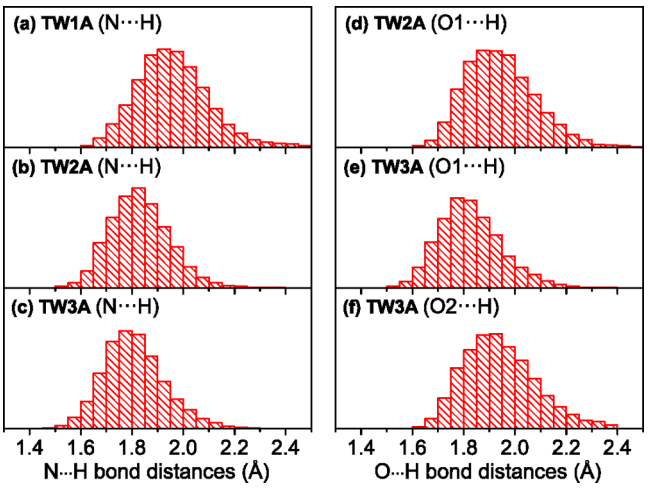

Figure 5. Normal distribution of N···H and O···H bond distances of isomers TW1A (250 K), TW2A (200 K), and TW3A (200 K) during AIMD simulations. The labels of the O, N, and H atoms in the structures are indicated in Figure 3.

Table 2. MP2/aug-cc-pVDZ Calculated Water Bending Overtones and HB-ed OH Stretches of the Most Stable Isomers of TMA$(H_2O)_n$ (n = 1−3; Frequencies, in cm^{-1})

isomer	$2\delta_{water\cdots O}$	$2\delta_{water\cdots N}$	$\nu^{HB}_{OH\cdots N}$	$\nu^{HB}_{OH\cdots O}$
TW1A		3200	3262	
TW2A	3172	3230	2990	3420
TW3A	3204	3246	2836	3397
	3164			3292

borrow the intensity from the H-bonded OH stretch. In the TW3A isomer, the mismatch in the frequency between $\nu^{HB}_{OH\cdots N}$ and $2\delta_{OH\cdots N}$ is 410 cm^{-1}, for which the OH bend overtone hardly borrows the intensity from the HB-ed OH stretch. These results indicate that the Fermi resonance between the HB-ed OH stretch fundamental (ν^{HB}_{OH}) and the OH bend overtone ($2\delta_{OH}$) plays a significant role in the dynamic couplings of H-bonds. The reason for this becomes apparent in the DOS plots of OH groups, as shown in Figure 6. The peak intensity of the O1H group that is connected to the N atom of TMA decreases with the increase of the water molecule. Consequently, the $\nu^{HB}_{OH\cdots N}$ band is broadened at n = 2 and smeared out at n = 3. As discussed previously,[23,34] the satisfactory agreement between experiment and theory for such floppy hydrated clusters is very difficult, because of the limitation of theoretical methods such as incomplete sampling of potential energy surfaces or neglected degrees of freedom.

The interaction of sulfur dioxide (SO_2) with water widely exists in atmospheric environments. Vibrational sum-frequency generation (SFG) spectroscopic studies of H_2O-interfacial SO_2 identified a $_{(SO_2)}O\cdots H_{(H_2O)}$ motif.[40−43] Born−Oppenheimer molecular dynamics (BOMD) simulations predicted that the $_{(SO_2)}S\cdots O_{(H2O)}$ motif is dominated in the gas phase, whereas the $_{(SO2)}O\cdots H_{(H_2O)}$ motif is favored on the water nanodroplet.[44] Spectroscopic investigation of size-selected $SO_2(H_2O)_n$ clusters by adding one water molecule at a time would help unravel the stepwise development of the hydration structures. Figure 7 shows the experimental IR-VUV depletion spectra of $SO_2(H_2O)_n$ with n = 1 through 16. The MP2/aug-cc-pVDZ calculations were carried out for the representative $SO_2(H_2O)_{1-8}$.[24] Figure 8 shows the most stable structures and their simulated spectra of n = 1−8.

The comparison of experimental and theoretical spectra assigns band A to the free OH stretch of H_2O that is bound to adjacent H_2O (abbreviated as OH^{free}_W), band B to the OH stretch of H_2O that is located in the $_{(SO_2)}O\cdots H_{(H_2O)}$ interaction ($OH^{SO\cdots HO}_S$), band C to the OH stretch of H_2O that is located in the $_{(SO_2)}S\cdots O_{(H_2O)}$ interaction ($OH^{OS\cdots OH}_S$), and band D to the HB-ed OH stretch of H_2O that is bound to adjacent H_2O (OH^{HB}_W), respectively. As shown in Figure 8, the most stable structure of $SO_2(H_2O)$ features a sandwich $_{(SO_2)}S\cdots O_{(H_2O)}$ motif. The most stable structures of n = 2 and 3 have cyclic two-dimensional (2D) geometries, in which the $_{(SO_2)}O\cdots H_{(H_2O)}$ and $_{(SO_2)}S\cdots O_{(H_2O)}$ motifs are formed. Starting at $SO_2(H_2O)_4$, three-dimensional cage structures are formed by keeping hold of the

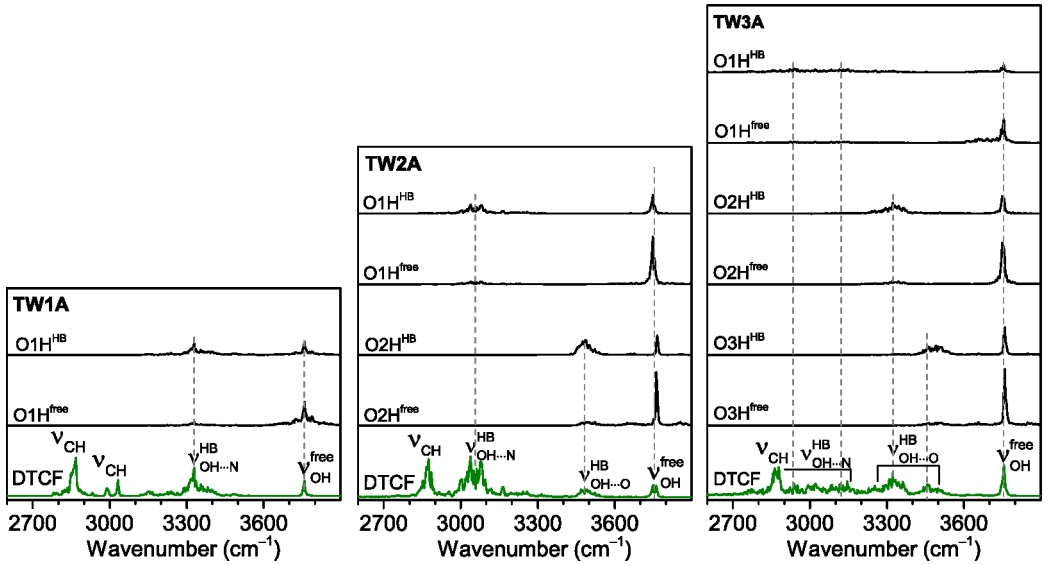

Figure 6. DTCF spectra (bottom row) and DOS plots of OH groups (upper rows) obtained from the AIMD simulations of isomers TW1A (250 K), TW2A (200 K), and TW3A (200 K).

https://doi.org/10.1021/acs.jpclett.4c00896
J. Phys. Chem. Lett. 2024, 15, 4806−4814

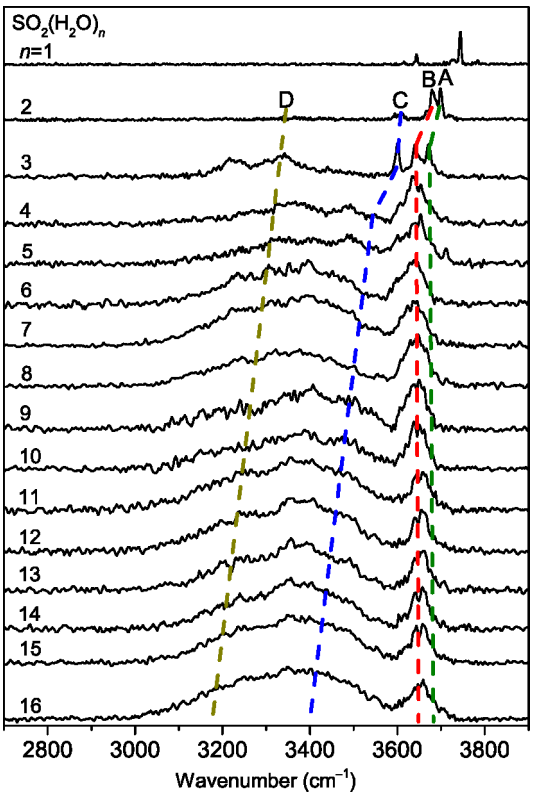

Figure 7. Experimental IR-VUV depletion spectra of $SO_2(H_2O)_n$ with n = 1 through 16.

$_{(SO_2)}O\cdots H_{(H_2O)}$ and $_{(SO_2)}S\cdots O_{(H_2O)}$ motifs. The observed motif evolution from $_{(SO2)}S\cdots O_{(H_2O)}$ to $_{(SO_2)}O\cdots H_{(H_2O)}$ verifies the BOMD predictions.[44] More detailed discussions could be found in our previous reports.[24]

Recently, VUV-FEL-based size-specific IR spectroscopic studies of water clusters have identified a few new structures for $(H_2O)_n$ (n = 5−10).[29−33] It would be of interest to look at the effect of SO_2 on the structures of these pure water clusters. SO_2 binds to the water dimer to form a 2D cyclic hydrate structure, which ring size increases in a larger cluster of $SO_2(H_2O)_3$. Consequently, the cyclic structure of $(H_2O)_3$ is opened by the SO_2. A 3D hydrate structure is formed in the $SO_2(H_2O)_4$ cluster, in which the original ring of $(H_2O)_4$ is not significantly affected by SO_2. It could be because the bond tension of the 2D cyclic hydrate structure of $SO_2(H_2O)_4$ is too large to be stabilized. Starting at $SO_2(H_2O)_6$, a cage hydrate structural motif is formed. SO_2 prefers to bind to the outer side of the cage structures of $(H_2O)_8$. Even though the SO_2 uptake would induce subtle perturbation to the structures of larger water systems, it could impact the electrophilicity and reactivity of SO_2 on the water nanodroplets and surfaces.

The interactions of metals with water are ubiquitous in many fields such as synthesis, electrochemical catalysis, and energy systems.[45,46] Molecular-level investigation of archetypal metal−water systems might provide insights into the fundamental reactions of the relevant processes. Recently, we have studied the reactions of neutral early transition metals with water using the VUV-FEL-based IR spectroscopy.[25−28] Figure 9 shows the experimental IR-VUV depletion spectra and identified structures of neutral $H^{\bullet}M(OH)_3$ and $H^{\bullet}M(OH)_3(H_2O)$ clusters (M = Sc, Y, La) formed from the reactions of group 3 metal atoms with water molecules. Detailed computational methods and

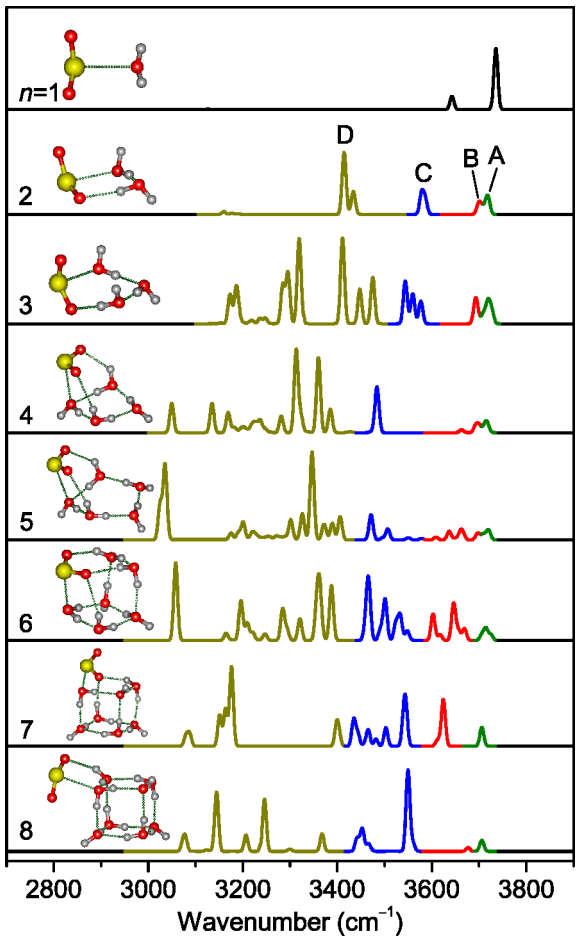

Figure 8. Simulated IR spectra of the most stable structures of $SO_2(H_2O)_n$ (n = 1−8) clusters. The colors of the S, O, and H atoms are indicated with yellow, red, and light gray, respectively.

spectral assignments could be found in previous reports.[25,28] Taking the Sc system as an example, the Mulliken spin density of $H^{\bullet}$ in $H^{\bullet}Sc(OH)_3$ and $H^{\bullet}Sc(OH)_3(H_2O)$ is calculated to be 0.76 and 0.72, respectively, indicative of a characteristic of the hydrogen radical; the IR spectral signature of the hydrogen radical features scaled calculated frequencies at 682 cm^{-1} (O−H wagging) and 811 cm^{-1} (Sc−H stretching), which are close to the limit of the IR wavelength range of LaserVision and expected to be measured by the intense and tunable IR free electron laser. The observation of $H^{\bullet}$ is quite intriguing in that its capture is extremely difficult due to its short lifetime and high reactivity.[47] The accomplishment of this target benefits from the efficient collisions of helium expansion in our recently developed cluster source and sensitive detection by VUV-FEL-based IR spectroscopy. These findings have important implications for the design and preparation of complexes with special structures and properties.

Figure 10 shows the experimental IR-VUV depletion spectra and identified structures of neutral $V_2O_3H_4$ and $V_2O_4H_6$ clusters generated from the reactions of vanadium dimers with water molecules. The $V_2O_3H_4$ and $V_2O_4H_6$ clusters are identified to have $V_2(\mu_2\text{-OH})(\mu_2\text{-H})(\eta^1\text{-OH})_2$ and $V_2(\mu_2\text{-OH})_2(\eta^1\text{-H})_2(\eta^1\text{-OH})_2$ structures, in which the water molecules are split. The exothermic value of the $V(^4F) + V(^4F) \rightarrow V_2(^3\Sigma_g^-)$ reaction (66.3 kcal/mol calculated at the BPW91/6-311++G(d,p) (O, H)/6-311G (V) level) is much larger than that of the $V(^4F)$ +

https://doi.org/10.1021/acs.jpclett.4c00896
J. Phys. Chem. Lett. 2024, 15, 4806−4814

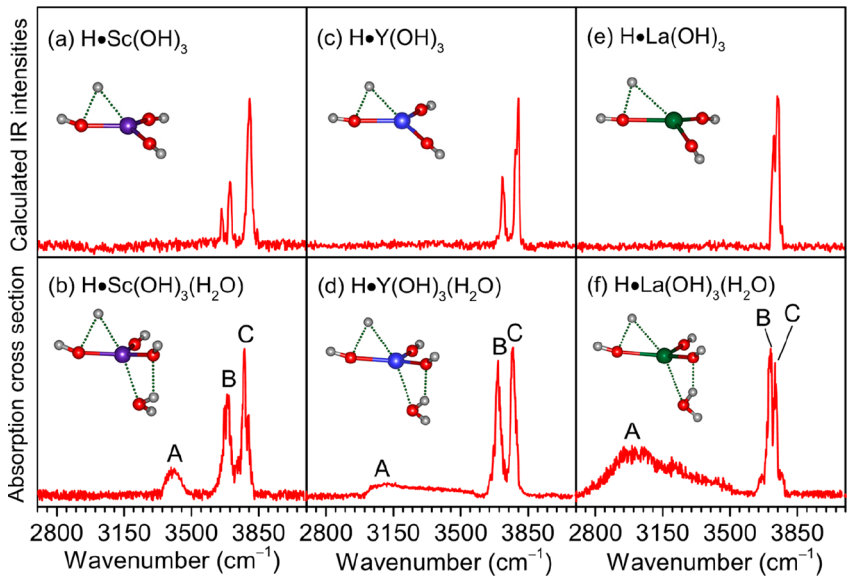

Figure 9. Experimental IR-VUV depletion spectra and identified structures of neutral $H^{\bullet}M(OH)_3$ and $H^{\bullet}M(OH)_3(H_2O)$ clusters (M = Sc, Y, La). Spectral assignments: the symmetric OH stretch of water (labeled A), antisymmetric OH stretch of water (labeled B), and OH stretch of hydroxy (labeled C). The colors of the Sc, Y, La, O, and H atoms are indicated with purple, blue, olive, red, and light gray, respectively.

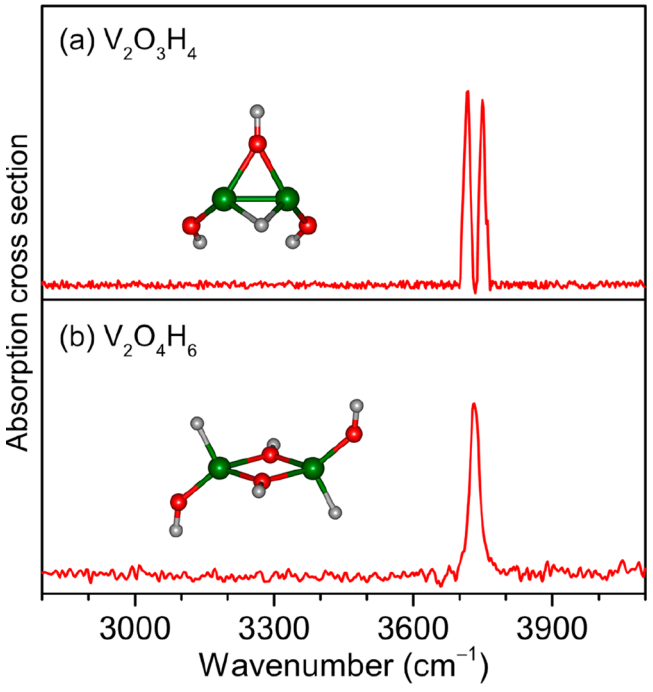

Figure 10. Experimental IR-VUV depletion spectra and identified structures of neutral $V_2O_3H_4$ and $V_2O_4H_6$ clusters (V, olive; O, red; H, light gray).

$H_2O(^1A_1) \rightarrow V(H_2O)(^4A')$ reaction (17.1 kcal/mol), indicating that the formation of V_2 is more favorable than that of $V(H_2O)$. Indeed, the mass spectral intensity of V_2^+ is much larger that of $V(H_2O)^+$ as reported previously.[27] The V_2 cluster reacts with H_2O and subsequently undergoes several reactions to form $V_2O_3H_4$ and $V_2O_4H_6$. Experimental and theoretical results show that water splitting by V_2 is both thermodynamically exothermic and kinetically facile in the gas phase.

This Perspective summarizes our recent progress in the VUV-FEL-based size-specific IR spectroscopic studies of neutral amine−water, sulfur dioxide−water, and metal−water clusters. Since the first ionization potentials of numerous neutral clusters fall in the tunable VUV-FEL wavelength region (50−150 nm/8.3−24.8 eV), threshold ionization detection of these clusters could be realized with this unique FEL source. Thus, the VUV-FEL-based size-specific IR spectroscopy should be generally applicable to many neutral clusters with efficient vibrational excitations accessible by tunable and intense infrared laser sources. Future VUV-FEL-based size-specific IR spectroscopic studies of several neutral cluster systems are proposed as follow.

(1) Structural evolution of neutral hydrated metal salt clusters. The dissolution of metal salts in water is a universal physicochemical process that is important in the chemical, biological, and atmospheric environment fields.[48] One key issue is how many water molecules are required to form a solvent-separated ion pair (SSIP). Several classes of ionic hydrated metal salt clusters have been studied experimentally and theoretically, which made considerable progresses in the solvation structures of individual ion pairs.[49−51] Future research is aimed to study the stepwise structures and properties of neutral hydrated metal salt clusters and to obtain microscopic dynamical images of metal salt dissolution processes in water.

(2) Structural evolution of neutral hydrated acid clusters. The acid dissociation is essential in homogeneous/heterogeneous reactions and biological and atmospheric processes.[52,53] The dissociation of HCl with four water molecules was suggested by superfluid He nanodroplet experiments.[54] Femtosecond pump−probe spectroscopic studies indicate that the dissociation of HBr needs at least five water molecules.[55] Infrared photodissociation spectroscopy of $Cs^+\cdot(HNO_3)(H_2O)_{n=0-11}$ reveals the formation of a SSIP $Cs^+-NO_3^-{-}H_3O^+$ salt bridge at $n = 10$. Future research would focus on the systematic studies of structural evolution of numerous neutral hydrated acid clusters.

(3) The reactions of metal cluster neutral metal atoms/clusters with small molecules. The single-atom/cluster

https://doi.org/10.1021/acs.jpclett.4c00896
J. Phys. Chem. Lett. 2024, 15, 4806−4814

catalysis has made substantial progresses in fundamental research and industrial applications.[56] Size-dependent studies on the reaction mechanisms of neutral metal atoms/clusters with a number of molecules (i.e., CO, CO_2, CH_4, C_3H_8, H_2O, N_2, NO, NO_2, NH_3, etc.) would help to provide microscopic insights into single-site reaction processes.

AUTHOR INFORMATION

Corresponding Authors

Gang Li − *State Key Laboratory of Molecular Reaction Dynamics and Dalian Coherent Light Source, Dalian Institute of Chemical Physics, Chinese Academy of Sciences, Dalian 116023, China;* orcid.org/0000-0001-5984-111X; Email: gli@dicp.ac.cn

Ling Jiang − *State Key Laboratory of Molecular Reaction Dynamics and Dalian Coherent Light Source, Dalian Institute of Chemical Physics, Chinese Academy of Sciences, Dalian 116023, China; Hefei National Laboratory, Hefei 230088, China;* orcid.org/0000-0002-8485-8893; Email: ljiang@dicp.ac.cn

Author

Hua Xie − *State Key Laboratory of Molecular Reaction Dynamics and Dalian Coherent Light Source, Dalian Institute of Chemical Physics, Chinese Academy of Sciences, Dalian 116023, China;* orcid.org/0000-0003-2091-6457

Complete contact information is available at: https://pubs.acs.org/10.1021/acs.jpclett.4c00896

Notes

The authors declare no competing financial interest.

Biographies

Gang Li is an associate professor of the State Key Laboratory of Molecular Reaction Dynamics, Dalian Institute of Chemical Physics (DICP), Chinese Academy of Sciences (CAS). He received his Ph.D. degree in 2015 from Dalian University of Technology. After a two year Lectureship at Henan University of Urban Construction, he moved to DICP. His research interest mainly focuses on the infrared spectroscopic studies of the structural evolution of atmospheric clusters.

Hua Xie is a full professor of the State Key Laboratory of Molecular Reaction Dynamics, DICP, CAS. He received his Ph.D. degree in 2013 from DICP, CAS. After graduation, he joined the State Key Laboratory of Molecular Reaction Dynamics, DICP. His research interest mainly focuses on the photoelectron velocity-map imaging spectroscopic and infrared photodissociation spectroscopic studies on the structures and reactivity of metal clusters.

Ling Jiang is a full professor of the State Key Laboratory of Molecular Reaction Dynamics, DICP, CAS. He received his Ph.D. from Kobe University, Japan, in 2007. He was a JSPS fellow at National Institute of Advanced Industrial Science and Technology (AIST), Japan, from 2007 to 2009. Then, he spent two years at Fritz-Haber-Institute of Max Planck Society, Germany, as an Alexander von Humboldt fellow. From 2011 to now, he has been working at DICP. His research is focused on the spectroscopic study of clusters and atmospheric aerosols.

ACKNOWLEDGMENTS

The authors greatly appreciate fruitful collaborations with outstanding colleagues (i.e., Professors Xueming Yang, Donghui Zhang, Jun Li, Zhaojun Zhang, Hongjun Fan, Zhifeng Liu, Jer-Lai Kuo, etc.) and the contributions of graduate students and postdoctoral fellows. This work was supported by the National Natural Science Foundation of China (NSFC) (22125303, 92361302, 92061203, 22103082, 22273101, and 21327901), the NSFC Center for Chemical Dynamics (22288201), the National Key Research and Development Program of China (2021YFA1400501), the Innovation Program for Quantum Science and Technology (2021ZD0303304), the Scientific Instrument Developing Project of the Chinese Academy of Sciences (GJJSTD20220001), the International Partnership Program of the Chinese Academy of Sciences (121421KYSB20170012), and Dalian Institute of Chemical Physics (DICP I202437).

REFERENCES

(1) Kulmala, M.; et al. Direct Observations of Atmospheric Aerosol Nucleation. *Science* **2013**, *339*, 943−946.
(2) Dai, S.; Funk, L.-M.; von Pappenheim, F. R.; Sautner, V.; Paulikat, M.; Schroder, B.; Uranga, J.; Mata, R. A.; Tittmann, K. Low-barrier Hydrogen Bonds in Enzyme Cooperativity. *Nature* **2019**, *573*, 609−613.
(3) Fujishima, A.; Honda, K. Electrochemical Photolysis of Water at a Demiconductor Electrode. *Nature* **1972**, *238*, 37−38.
(4) Buck, U.; Huisken, F. Infrared Spectroscopy of Size-Selected Water and Methanol Clusters. *Chem. Rev.* **2000**, *100*, 3863−3890.
(5) Robertson, W. H.; Johnson, M. A. Molecular Aspects of Halide Ion Hydration: The Cluster Approach. *Annu. Rev. Phys. Chem.* **2003**, *54*, 173−213.
(6) Fujii, A.; Mizuse, K. Infrared Spectroscopic Studies on Hydrogen-Bonded Water Networks in Gas Phase Clusters. *Int. Rev. Phys. Chem.* **2013**, *32*, 266−307.
(7) Potapov, A.; Asselin, P. High-Resolution Jet Spectroscopy of Weakly Bound Binary Complexes Involving Water. *Int. Rev. Phys. Chem.* **2014**, *33*, 275−300.
(8) Heine, N.; Asmis, K. R. Cryogenic Ion Trap Vibrational Spectroscopy of Hydrogen-Bonded Clusters Relevant to Atmospheric Chemistry. *Int. Rev. Phys. Chem.* **2015**, *34*, 1−34.
(9) Heine, N.; Yacovitch, T. I.; Schubert, F.; Brieger, C.; Neumark, D. M.; Asmis, K. R. Infrared Photodissociation Spectroscopy of Micro-hydrated Nitrate-Nitric Acid Clusters $NO_3^-(HNO_3)_m(H_2O)_n$. *J. Phys. Chem. A* **2014**, *118*, 7613−7622.
(10) Sun, S.-T.; Jiang, L.; Liu, J. W.; Heine, N.; Yacovitch, T. I.; Wende, T.; Asmis, K. R.; Neumark, D. M.; Liu, Z.-F. Microhydrated Dihydrogen Phosphate Clusters Probed by Gas Phase Vibrational Spectroscopy and First Principles Calculations. *Phys. Chem. Chem. Phys.* **2015**, *17*, 25714−25724.
(11) Henderson, B. V.; Jordan, K. D. One-Dimensional Adiabatic Model Approach for Calculating Progressions in Vibrational Spectra of Ion-Water Complexes. *J. Phys. Chem. A* **2019**, *123*, 7042−7050.
(12) Chatterjee, K.; Dopfer, O. Microhydration of Protonated Biomolecular Building Blocks: Protonated Pyrimidine. *Phys. Chem. Chem. Phys.* **2020**, *22*, 13092−13107.
(13) Whittle, E.; Dows, D. A.; Pimentel, G. C. Matrix Isolation Method for the Experimental Study of Unstable Species. *J. Chem. Phys.* **1954**, *22*, 1943−1943.
(14) Balle, T. J.; Flygare, W. H. Fabry-Perot Cavity Pulsed Fourier Transform Microwave Spectrometer with a Pulsed Nozzle Particle Source. *Rev. Sci. Instrum.* **1981**, *52*, 33−45.
(15) Brown, G. G.; Dian, B. C.; Douglass, K. O.; Geyer, S. M.; Shipman, S. T.; Pate, B. H. A Broadband Fourier Transform Microwave Spectrometer Based on Chirped Pulse Excitation. *Rev. Sci. Instrum.* **2008**, *79*, 053103.
(16) Cohen, R. C.; Saykally, R. J. Vibration-Rotation-Tunneling Spectroscopy of the van der Waals Bond: A New Look at Intermolecular Forces. *J. Phys. Chem.* **1992**, *96*, 1024−1040.
(17) Goyal, S.; Schutt, D. L.; Scoles, G. Vibrational Spectroscopy of Sulfur Hexafluoride Attached to Helium Clusters. *Phys. Rev. Lett.* **1992**, *69*, 933−936.
(18) Buck, U.; Meyer, H. Scattering Analysis of Cluster Beams: Formation and Fragmentation of Small Ar_n Clusters. *Phys. Rev. Lett.* **1984**, *52*, 109−112.
(19) Normile, D. Unique Free Electron Laser Laboratory Opens in China. *Science* **2017**, *355*, 235−235.
(20) Zhang, B.; et al. Infrared Spectroscopy of Neutral Water Dimer Based on a Tunable Vacuum Ultraviolet Free Electron Laser. *J. Phys. Chem. Lett.* **2020**, *11*, 851−855.
(21) Li, G.; et al. Infrared plus Vacuum Ultraviolet Two-Color Ionization Spectroscopy of Neutral Metal Complexes based on a Tunable Vacuum Ultraviolet Free-Electron Laser. *Rev. Sci. Instrum.* **2020**, *91*, 034103.
(22) Li, G.; Wang, C.; Zheng, H.-J.; Wang, T.-T.; Xie, H.; Yang, X.-M.; Jiang, L. Infrared Spectroscopy of Neutral Clusters based on a Vacuum Ultraviolet Free Electron Laser. *Chin. J. Chem. Phys.* **2021**, *34*, 51−60.
(23) Jiang, S.; et al. Vibrational Signature of Dynamic Coupling of a Strong Hydrogen Bond. *J. Phys. Chem. Lett.* **2021**, *12*, 2259−2265.
(24) Wang, C.; et al. Infrared Spectroscopy of Stepwise Hydration Motifs of Sulfur Dioxide. *J. Phys. Chem. Lett.* **2022**, *13*, 5654−5659.
(25) Jiang, S.; et al. Capturing Hydrogen Radicals by Neutral Metal Hydroxides. *J. Phys. Chem. Lett.* **2023**, *14*, 2481−2486.
(26) Jiang, S.; et al. Spectroscopic Identification of Water Splitting by Neutral Group 3 Metals. *Chin. Chem. Lett.* **2023**, *34*, 108244.
(27) Zheng, H.; Jiang, S.; Yan, W.; Wang, T.; Li, S.; Xie, H.; Li, G.; Yang, X.; Jiang, L. Size-Specific Infrared Spectroscopic Study of the Reactions between Water Molecules and Neutral Vanadium Dimer: Evidence for Water Splitting. *J. Phys. Chem. Lett.* **2023**, *14*, 3878−3883.
(28) Wang, T.; Li, S.; Yan, W.; Jiang, S.; Xie, H.; Li, G.; Jiang, L. Infrared Spectroscopic Study of Solvation and Size Effects on Reactions between Water Molecules and Neutral Rare-Earth Metals. *Nanoscale Adv.* **2023**, *5*, 6626−6634.
(29) Zhang, B.; et al. Infrared Spectroscopy of Neutral Water Clusters at Finite Temperature: Evidence for a Noncyclic Pentamer. *Proc. Natl. Acad. Sci. U. S. A.* **2020**, *117*, 15423−15428.
(30) Li, G.; et al. Infrared Spectroscopic Study of Hydrogen Bonding Topologies in the Smallest Ice Cube. *Nat. Commun.* **2020**, *11*, 5449.
(31) Zhang, Y.-Y.; et al. Infrared Spectroscopic Signature of the Structural Diversity of the Water Heptamer. *Cell Rep. Phys. Sci.* **2022**, *3*, 100748.
(32) Zheng, H.; et al. Spectroscopic Snapshot for Neutral Water Nonamer $(H_2O)_9$: Adding A H_2O onto A Hydrogen Bond-Unbroken Edge of $(H_2O)_8$. *J. Chem. Phys.* **2023**, *158*, 014301.
(33) Zhang, Y.-Y.; et al. Spectroscopic and Theoretical Identifications of Two Structural Motifs of (H2O)10 Cluster. *J. Phys. Chem. Lett.* **2024**, *15*, 3055−3060.
(34) Zhang, B.; Yang, S.; Huang, Q.-R.; Jiang, S.; Chen, R.; Yang, X.; Zhang, D. H.; Zhang, Z.; Kuo, J.-L.; Jiang, L. Deconstructing Vibrational Motions on the Potential Energy Surfaces of Hydrogen-Bonded Complexes. *CCS Chem.* **2021**, *3*, 829−835.
(35) Wang, C.; et al. Observation of Carbon-Carbon Coupling Reaction in Neutral Transition-Metal Carbonyls. *J. Phys. Chem. Lett.* **2021**, *12*, 1012−1017.
(36) Zhao, Y.; et al. Ligand-Induced Tuning of the Electronic Structure of Rhombus Tetraboron Cluster. *ChemPhysChem* **2022**, *23*, No. e202200060.
(37) Wang, C.; et al. Observation of Confinement-Free Neutral Group Three Transition Metal Carbonyls $Sc(CO)_7$ and $TM(CO)_8$ (TM = Y, La). *Angew. Chem., Int. Ed.* **2023**, *62*, No. e202305490.
(38) Wang, T.; Zhang, Z.; Jiang, S.; Yan, W.; Li, S.; Zhuang, J.; Xie, H.; Li, G.; Jiang, L. Spectroscopic Characterization of Carbon Monoxide Activation by Neutral Chromium Carbides. *Phys. Chem. Chem. Phys.* **2024**, *26*, 5962−5968.
(39) Zhang, R.; Khalizov, A.; Wang, L.; Hu, M.; Xu, W. Nucleation and Growth of Nanoparticles in the Atmosphere. *Chem. Rev.* **2012**, *112*, 1957−2011.
(40) Ota, S. T.; Richmond, G. L. Uptake of SO_2 to Aqueous Formaldehyde Surfaces. *J. Am. Chem. Soc.* **2012**, *134*, 9967−9977.
(41) Ota, S. T.; Richmond, G. L. Chilling Out: A Cool Aqueous Environment Promotes the Formation of Gas-Surface Complexes. *J. Am. Chem. Soc.* **2011**, *133*, 7497−7508.
(42) Tarbuck, T. L.; Richmond, G. L. Adsorption and Reaction of CO_2 and SO_2 at a Water Surface. *J. Am. Chem. Soc.* **2006**, *128*, 3256−3267.
(43) Tarbuck, T. L.; Richmond, G. L. SO_2: H_2O Surface Complex Found at the Vapor/Water Interface. *J. Am. Chem. Soc.* **2005**, *127*, 16806−16807.
(44) Zhong, J.; Zhu, C.; Li, L.; Richmond, G. L.; Francisco, J. S.; Zeng, X. C. Interaction of SO2 with the Surface of a Water Nanodroplet. *J. Am. Chem. Soc.* **2017**, *139*, 17168−17174.
(45) Bjornehohn, E.; et al. Water at Interfaces. *Chem. Rev.* **2016**, *116*, 7698−7726.
(46) Ali, A.; Long, F.; Shen, P. K. Innovative Strategies for Overall Water Splitting Using Nanostructured Transition Metal Electro-catalysts. *Electrochem. Energy Rev.* **2022**, *5*, 1.

https://doi.org/10.1021/acs.jpclett.4c00896
J. Phys. Chem. Lett. 2024, 15, 4806−4814

(47) Buenermann, O.; Jiang, H.; Dorenkamp, Y.; Kandratsenka, A.; Janke, S. M.; Auerbach, D. J.; Wodtke, A. M. Electron-Hole Pair Excitation Determines the Mechanism of Hydrogen Atom Adsorption. *Science* **2015**, *350*, 1346−1349.
(48) Knipping, E. M.; Lakin, M. J.; Foster, K. L.; Jungwirth, P.; Tobias, D. J.; Gerber, R. B.; Dabdub, D.; Finlayson-Pitts, B. J. Experiments and Simulations of Ion-Enhanced Interfacial Chemistry on Aqueous NaCl Aerosols. *Science* **2000**, *288*, 301−306.
(49) Wang, X.-B.; Woo, H.-K.; Jagoda-Cwiklik, B.; Jungwirth, P.; Wang, L.-S. First Steps towards Dissolution of $NaSO_4^-$ by Water. *Phys. Chem. Chem. Phys.* **2006**, *8*, 4294−4296.
(50) Li, R.-Z.; Liu, C.-W.; Gao, Y. Q.; Jiang, H.; Xu, H.-G.; Zheng, W.-J. Microsolvation of LiI and CsI in Water: Anion Photoelectron Spectroscopy and ab initio Calculations. *J. Am. Chem. Soc.* **2013**, *135*, 5190−5199.
(51) Jiang, L.; Wende, T.; Bergmann, R.; Meijer, G.; Asmis, K. R. Gas-Phase Vibrational Spectroscopy of Microhydrated Magnesium Nitrate Ions $MgNO_3(H_2O)_{1-4}^+$. *J. Am. Chem. Soc.* **2010**, *132*, 7398−7404.
(52) Huthwelker, T.; Ammann, M.; Peter, T. The Uptake of Acidic Gases on Ice. *Chem. Rev.* **2006**, *106*, 1375−1444.
(53) Samanta, A. K.; Wang, Y.; Mancini, J. S.; Bowman, J. M.; Reisler, H. Energetics and Predissociation Dynamics of Small Water, HCl, and Mixed HCl-Water Clusters. *Chem. Rev.* **2016**, *116*, 4913−4936.
(54) Gutberlet, A.; Schwaab, G.; Birer, O.; Masia, M.; Kaczmarek, A.; Forbert, H.; Havenith, M.; Marx, D. Aggregation-Induced Dissociation of $HCl(H_2O)_4$ Below 1 K: The Smallest Droplet of Acid. *Science* **2009**, *324*, 1545−1548.
(55) Hurley, S. M.; Dermota, T. E.; Hydutsky, D. P.; Castleman, A. W. Dynamics of Hydrogen Bromide Dissolution in the Ground and Excited States. *Science* **2002**, *298*, 202−204.
(56) Qiao, B.; Wang, A.; Yang, X.; Allard, L. F.; Jiang, Z.; Cui, Y.; Liu, J.; Li, J.; Zhang, T. Single-Atom Catalysis of CO Oxidation using Pt_1/FeO_x. *Nat. Chem.* **2011**, *3*, 634−641.

https://doi.org/10.1021/acs.jpclett.4c00896
J. Phys. Chem. Lett. 2024, 15, 4806−4814